SUN Regulates Vegetative and Reproductive Organ Shape by Changing Cell Division Patterns[1][C][W][OA]

Shan Wu, Han Xiao[2], Antonio Cabrera, Tea Meulia, and Esther van der Knaap*

Department of Horticulture and Crop Science (S.W., H.X., A.C., E.v.d.K.) and Molecular and Cellular Imaging Center (T.M.), Ohio State University/Ohio Agricultural Research and Development Center, Wooster, Ohio 44691

One of the major genes controlling the elongated fruit shape of tomato (*Solanum lycopersicum*) is *SUN*. In this study, we explored the roles of *SUN* in vegetative and reproductive development using near isogenic lines (NILs) that differ at the *sun* locus, and *SUN* overexpressors in both the wild species LA1589 (*Solanum pimpinellifolium*) and the cultivar Sun1642 background. Our results demonstrate that *SUN* controls tomato shape through redistribution of mass that is mediated by increased cell division in the longitudinal and decreased cell division in the transverse direction of the fruit. The expression of *SUN* is positively correlated with slender phenotypes in cotyledon, leaflet, and floral organs, an elongated ovary, and negatively correlated with seed weight. Overexpression of *SUN* leads to more extreme phenotypes than those shown in the NILs and include thinner leaf rachises and stems, twisted leaf rachises, increased serrations of the leaflets, and dramatically increased elongation at the proximal end of the ovary and fruit. In situ hybridizations of the NILs showed that *SUN* is expressed throughout the ovary and young fruit, particularly in the vascular tissues and placenta surface, and in the ovules and developing seed. The phenotypic effects resulting from high expression of *SUN* suggest that the gene is involved in several plant developmental processes.

Tomato (*Solanum lycopersicum*) accessions feature a variety of fruit shapes and sizes (Paran and van der Knaap, 2007). Genes controlling fruit morphology offer important insights into the patterning of the organ and mechanisms by which organ shape and size are realized. One of the major tomato fruit shape genes is *SUN*, which, when expressed at high levels in the fruit, leads to an elongated shape (Xiao et al., 2008). The mutation that led to the identification of *SUN* was a gene duplication event mediated by the retrotransposon, *Rider*. The duplicated gene was placed in a novel genome environment, leading to high expression in the fruit (Xiao et al., 2008; Jiang et al., 2009). When overexpressing *SUN* under the control of the cauliflower mosaic virus 35S promoter in tomato, the transgenic plants produce extremely elongated and often seedless fruits (Xiao et al., 2008). *SUN* encodes a protein belonging to the IQD family and is characterized by the conserved IQ67 motif that is involved in calmodulin binding (Abel et al., 2005; Levy et al., 2005; Xiao et al., 2008). The function of this family of proteins is poorly understood. Overexpression of the Arabidopsis (*Arabidopsis thaliana*) gene *AtIQD1* increases the production of the secondary metabolite glucosinolate (Levy et al., 2005), whereas the high expression of *SUN* leads to elongated fruit shape. However, the biochemical mechanisms by which these phenotypes are realized are unknown. Moreover, gene expression studies in tomato did not show dramatic differences in the tomato with or without *SUN* (Xiao et al., 2009). Yet, the parthenocarpic fruit development associated with *SUN* overexpression led us to hypothesize that *SUN* may be involved in the production of a hormone or secondary metabolite that affects the auxin pathway either directly or indirectly (Xiao et al., 2008).

It has been hypothesized more than 200 years ago that carpels are modified leaves (Goethe, 1970; Coen, 2001). The notion has gained strong support from studies on flower and fruit development, indicating that floral organs and leaves are partly interchangeable through modifying only a small set of regulatory genes (Honma and Goto, 2001; Pelaz et al., 2001; Alonso-Cantabrana et al., 2007; Østergaard, 2009). Several tomato genes known for their roles in fruit set and growth also exert effects on leaf morphology (Jones

[1] This work was supported by the U.S. Department of Agriculture (grant no. 2007–35304–18295) and the National Science Foundation (grant no. DBI 0227541).

[2] Present address: Institute of Plant Physiology and Ecology, Shanghai Institutes for Biological Sciences, Chinese Academy of Sciences, Shanghai 200032, China.

* Corresponding author; e-mail vanderknaap.1@osu.edu.

The author responsible for distribution of materials integral to the findings presented in this article in accordance with the policy described in the Instructions for Authors (www.plantphysiol.org) is: Esther van der Knaap (vanderknaap.1@osu.edu).

[C] Some figures in this article are displayed in color online but in black and white in the print edition.

[W] The online version of this article contains Web-only data.

[OA] Open Access articles can be viewed online without a subscription.

www.plantphysiol.org/cgi/doi/10.1104/pp.111.181065

 © 2011 American Society of Plant Biologists. All Rights Reserved.

et al., 2002; Wang et al., 2005; de Jong et al., 2009b; Molesini et al., 2009). However, it is not clear whether, in addition to fruit shape, *SUN* also affects the phenotype of vegetative parts of tomato.

In this study, we evaluated the vegetative and reproductive phenotypes of the near isogenic lines (NILs) that differ at the *sun* locus as well as lines overexpressing *SUN* under the control of the 35S promoter in two genetic backgrounds: LA1589 (*Solanum pimpinellifolium*) and Sun1642 (tomato). Our results show that *SUN* has no significant effects on fruit weight, and that it regulates tomato fruit shape by rearrangement of fruit mass via an altered cell division pattern. In addition to fruit shape, *SUN* also controls floral organ and leaf morphology. High expression of *SUN* led to slender lateral organ shape, as well as thinner leaf rachis and stem. The involvement of *SUN* in multiple developmental processes suggests it may play a role in the basic programs of plant growth.

RESULTS

SUN Controls Fruit Shape by Rearranging Fruit Mass

NILs that differ at *sun* in both the LA1589 and the Sun1642 backgrounds showed a noticeable difference in fruit shape (Fig. 1). Sun1642ee and LA1589ee carry the gene duplication and produce elongated fruits, while Sun1642pp and LA1589pp are wild type at the locus and carry round fruits. Overexpression of *SUN* under the control of the 35S promoter in the round-fruited background (Sun1642ox and LA1589ox) led to extremely elongated fruit shape. The parthenocarpic

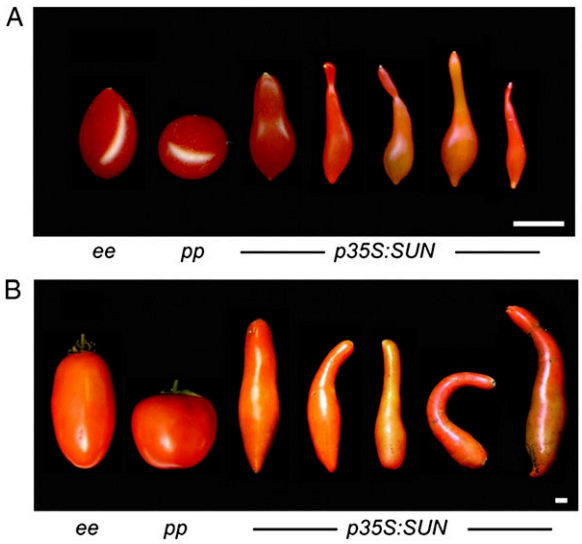

Figure 1. Fruit morphology of the *sun* NILs and overexpressors. A, Mature fruits from the *sun* NILs and five *SUN* overexpressors in LA1589 background. B, Mature fruits of the *sun* NILs and five *SUN* overexpressors in Sun1642 background. Scale bars: 1 cm. [See online article for color version of this figure.]

fruits from the overexpressors exhibited unusual proximal end elongation and often a pronounced tip (Fig. 1). To determine whether differences in fruit shape were accompanied by differences in fruit weight, seed weight, and seed number, we evaluated these traits in the NILs in both field- and greenhouse-grown plants. These traits were not evaluated in the lines that express *SUN* under the control of the 35S promoter because of the often seedless nature of these fruit and the irregular fruit set. Fruit weight and seed number per fruit did not differ significantly between the NILs in both the LA1589 and Sun1642 backgrounds, despite environmental effects (note that the differences between experiments were significant). This result indicated that the difference in fruit shape controlled by *SUN* was neither due to changes in seed number nor changes in fruit weight. Seed weight on the other hand differed between the NILs but only consistently in the LA1589 background (Table I). This result suggested that *SUN* might control seed development in addition to fruit shape. However, the effect on seed weight could also be due to other genes at the locus that are differentially expressed, for example *DEFL1* (Xiao et al., 2008). To evaluate whether *SUN* itself affected seed weight, transgenic lines that express *SUN* under its own promoter were evaluated. From six independent transgenic lines, three appeared to show a reduction in seed weight compared to control albeit that this was only significant in one transgenic line (Supplemental Table S1).

Since fruit weight was not affected by *SUN*, we hypothesized that shape was controlled by the rearrangement of fruit mass. To explore the tissue and cellular basis of the mass rearrangement, we evaluated the length, width, and thickness of the pericarp and septum, as well as cell number and cell size in these tissues. Fruits were collected from *sun* NILs in LA1589 background at 7 DPA. At this time point, the fruit shape index (length/width ratio) difference between the NILs is at the maximum level (Xiao et al., 2009). A difference was found in septum morphology such that the septum of LA1589ee was much more elongated and narrower than LA1589pp (Fig. 2A; Table II). In LA1589ee, more cells were found in the longitudinal direction of the septum and less cells in the transverse direction compared to LA1589pp. On the other hand, septum cell size was not significantly altered between the NILs (Fig. 2A; Table II). With respect to the pericarp, the longitudinal perimeter and the number of cells in this dimension were increased in LA1589ee, whereas cell size was not. In the transverse direction, cell number along the perimeter was not significantly different, and the increased pericarp perimeter in LA1589pp was due to the enlarged mesocarp cell size (Table II). This finding was supported by the notion that while the pericarp was slightly thicker in LA1589pp than in LA1589ee, the number of cell layers was not altered and therefore cell size was altered to account for difference in thickness. It should be noted that at this stage in fruit, mesocarp cell size increases

Table I. *Comparison of fruit weight, seed number, and seed weight in the sun NILs*

Traits	*N*	LA1589 NILs		*N*	Sun1642 NILs	
		F Value	*P* Value		*F* Value	*P* Value
Fruit weight	45			47		
Genotype		3.38	0.077		0.02	0.901
Replicate		38.98	<0.0001		30.84	<0.0001
Genotype × replicate		0.12	0.7358		0.23	0.632
Seed no.	45			38		
Genotype		0.86	0.360		2.74	0.107
Replicate		6.33	0.016		13.38	0.001
Genotype × replicate		0.47	0.495		0.95	0.336
Seed weight	95			68		
Genotype		48.95	<0.0001		0.58	0.451
Replicate		10.64	0.002		11.92	0.001
Genotype × replicate		0.09	0.764		6.78	0.012

dramatically (Xiao et al., 2009). We cannot rule out the possibility that the differences in cell size of the mesocarp cells in the transverse direction is due to slightly slower fruit development in LA1589ee compared to LA1589pp. Regardless, these results indicated that the largest change in fruit ontogeny arose from changes in cell proliferation, resulting in a significantly higher number of cells in the longitudinal direction and less cells in the transverse plane.

Since ovary shape is already slightly different at the time of anthesis (Xiao et al., 2008), we evaluated whether changes in cell morphology were detected at that time. The analyses were based on three ovaries sectioned longitudinally, through the center, and five ovaries sectioned transversely through the center for each genotype. The ovary length and width, and the septum length were significantly different between LA1589ee and LA1589pp (Supplemental Table S2). Although the differences in cell size and the number of cells along the longitudinal direction were not significant, we noticed a trend of more cells in the longitudinal direction of LA1589ee septum (Supplemental Table S2). Similar to 7-DPA fruit, distal and proximal end areas were also longer in LA1589ee compared to

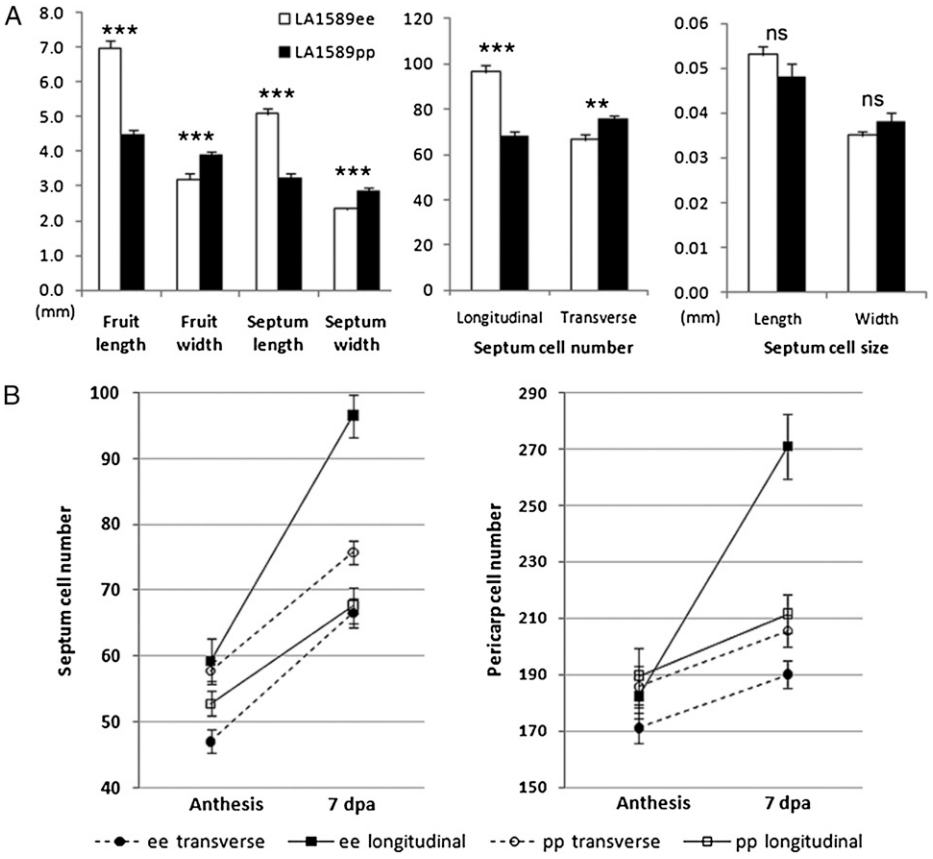

Figure 2. Cell morphology in the fruits of the LA1589 NILs that differ at *sun*. A, Fruit length, width, and septum morphology of fruit at 7 DPA. B, Increases of cell number in the septa and pericarps from anthesis to 7 DPA. **, $P < 0.01$; ***, $P < 0.001$; ns, not significant.

Table II. *Scanning electron microscopy analysis of 7-DPA fruits from the LA1589 sun NILs*

Each value (mean ± SE) represents eight longitudinally cut fruits or eight transversely cut fruits. *P* values were calculated from Student's *t* test.

Traits	LA1589ee	LA1589pp	*P*
Septum			
Fruit length (mm)	6.965 ± 0.236	4.478 ± 0.156	<0.0001
Fruit width (mm)	3.190 ± 0.162	3.876 ±0.117	0.0003
Septum length (mm)	5.087 ± 0.157	3.238 ± 0.133	<0.0001
Septum cell length (mm)	0.053 ± 0.002	0.048 ± 0.003	0.2141
Septum cell no. – longitudinal	96.5 ± 3.3	67.7 ± 2.7	<0.0001
Septum width (mm)	2.346 ± 0.039	2.847 ± 0.090	0.0004
Septum cell width (mm)	0.035 ± 0.001	0.038 ± 0.002	0.2542
Septum cell no. – transverse	66.6 ± 2.3	75.7 ± 1.8	0.0050
No. of cell layers in septum	8.0 ± 0.3	9.1 ± 0.3	0.8530
Pericarp			
Pericarp perimeter – longitudinal (mm)	16.384 ± 0.384	13.752 ± 0.564	0.0017
Mesocarp cell length (mm)	0.061 ± 0.003	0.065 ± 0.002	0.3570
Cell no. along the perimeter – longitudinal[a]	270.9 ± 11.6	211.5 ± 6.8	0.0009
Pericarp perimeter – transverse (mm)	10.805 ± 0.127	13.212 ± 0.445	0.0004
Pericarp thickness (mm)	0.431 ± 0.011	0.494 ± 0.013	0.0023
Mesocarp cell width (mm)	0.057 ± 0.001	0.064 ± 0.002	0.0086
Cell no. along the perimeter – transverse[a]	190.0 ± 4.9	205.491 ± 5.8	0.0741
No. of cell layers in pericarp	14.0 ± 0.3	13.8 ± 0.2	0.4291
Distal and proximal ends			
Distal end length (mm)	0.659 ± 0.025	0.513 ± 0.015	0.0003
Distal end cell length (mm)	0.049 ± 0.005	0.037 ± 0.003	0.0729
Distal end cell no.	14.6 ± 1.7	14.3 ± 1.4	0.8837
Proximal end length (mm)	1.025 ± 0.071	0.803 ± 0.055	0.0315
Proximal end cell length (mm)	0.049 ± 0.002	0.042 ± 0.001	0.0032
Proximal end cell no.	21.3 ± 1.8	19.4 ± 1.5	0.4522

[a]Numbers of cells along the perimeter were estimated based on mesocarp size and perimeter length.

LA1589pp ovaries at anthesis (Table II; Supplemental Table S2). The septum cell number in the transverse direction was significantly higher in LA1589pp, but this was offset by reduction in cell size, leading to equal septum width in both NILs (Supplemental Table S2). Nevertheless, this result indicated that reduced cell number in the transverse direction of LA1589ee septum was already observed in anthesis-stage ovaries.

To evaluate further whether changes in cell division occurred prior to or after pollination, we compared septum and pericarp morphology at anthesis and 7 DPA. In the longitudinal direction, septum cell number increased 63% from anthesis to 7 DPA in LA1589ee and only 28% in LA1589pp (Fig. 2B). Similarly, in the pericarp, cell number increased 49% and 12% in LA1589ee and LA1589pp, respectively. In the transverse direction, differences in cell number were observed as early as at anthesis, and transverse cell number increases in septum and pericarp after anthesis until 7 DPA were comparable in both NILs (Fig. 2B). This result suggested that while changes in cell division along the medio-lateral axis were already executed at the time of anthesis, changes in cell division along the apical-basal axis were executed shortly after pollination. In sum, the changes in the direction of cell division in septum and pericarp led to a greatly elongated fruit shape (Fig. 1).

Mutually Exclusive Expression Patterns of *SUN* and *DEFL1*

To investigate the tissue-specific expression of *SUN*, we performed RNA in situ hybridization in ovaries and young fruits of *sun* NILs in the LA1589 background. We also analyzed the expression pattern of *DEFL1*, a gene that is expressed in round fruit but not in elongated fruit due to the gene duplication event at the locus (Xiao et al., 2008). In addition to using *DEFL1* as control probe for hybridization (we expected no hybridization of *DEFL1* when *SUN* is expressed and vice versa) we wanted to test the hypothesis that the promoter of *DEFL1* is driving expression of *SUN*, which would be consistent with previous findings (Xiao et al., 2008). To visualize the internal structure along different axes, hybridizations of *SUN* and *DEFL1* were conducted using longitudinally cut sections as well as transverse sections. *SUN* was expressed in LA1589ee, but barely detected in LA1589pp (Fig. 3, A, C, and E). Conversely, *DEFL1* transcript was only accumulating in LA1589pp (Fig. 3, B, D, and F). At 2 d before anthesis, *SUN* was highly expressed in vascular tissues and embryo sac of the ovule (Fig. 3A). At anthesis and 2 DPA at the onset of embryo development (Xiao et al., 2009), *SUN* transcript was localized in the vascular tissues of the sepals and most parts of the ovary, including ovary wall, placenta surface, and seed (Fig. 3, C and E). The central region

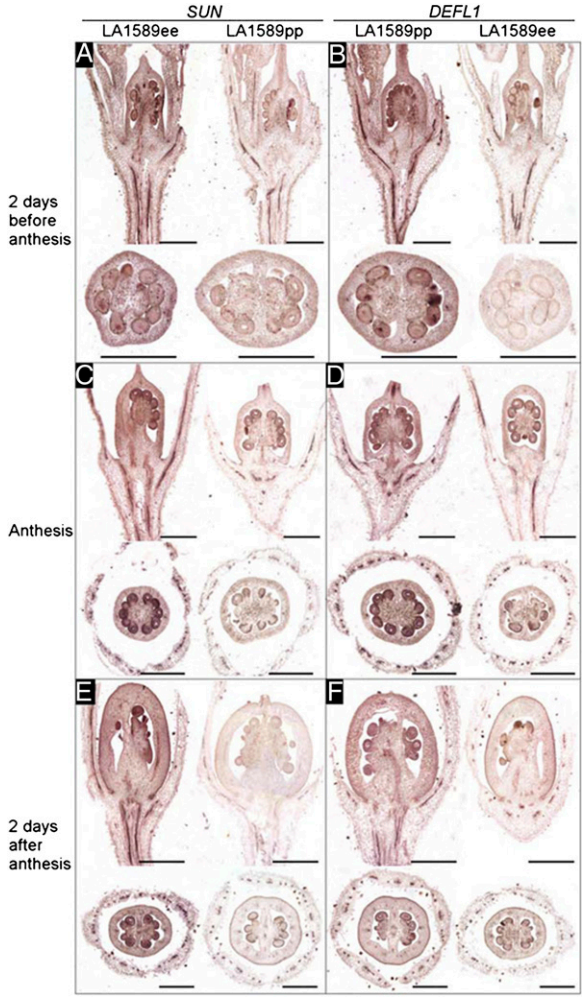

Figure 3. Expressions of *SUN* and *DEFL1* mRNA in ovaries and young fruits of *sun* NILs in the LA1589 background. A, Two days before anthesis ovaries hybridized with *SUN* antisense probe. B, Two days before anthesis ovaries hybridized with *DEFL1* antisense probe. C, Anthesis ovaries hybridized with *SUN* antisense probe. D, Anthesis ovaries hybridized with *DEFL1* antisense probe. E, Two days postanthesis fruits hybridized with *SUN* antisense probe. F, Two days postanthesis fruits hybridized with *DEFL1* antisense probe. Longitudinal sections and cross sections are located at the top and bottom parts, respectively. Scale bars: 500 μm.

of the columella had relatively low signals except for where the vascular bundles are located (Fig. 3, A, C, and E). At 6 d after fertilization when the embryo is at the globular stage (Xiao et al., 2009), high levels of *SUN* transcript were found in the pericarp and developing embryo of LA1589ee (Supplemental Fig. S1). The dark staining in septum and the inner layers of pericarp was due to the accumulation of starch grains (Supplemental Fig. S1, inserts). At all of these stages, the expression patterns of *DEFL1* in LA1589pp ovary and fruit mirrored those of *SUN* in LA1589ee (Fig. 3; Supplemental Fig. S1).

The expression of *SUN* and *DEFL1* in vegetative parts and floral organs was also analyzed by northern blot. At the time of anthesis, the highest levels of *SUN* transcript in flower were found in sepals, petals, and ovaries of LA1589ee and Sun1642ee (Fig. 4A). *DEFL1*, on the other hand, showed highest expression in the same organs of LA1589pp and Sun1642pp, and was barely detected in LA1589ee and Sun1642ee. Different vegetative tissues were collected from young seedlings at 7 d after germination. We found *SUN* was expressed the highest in hypocotyl and shoot apex of LA1589ee and Sun1642ee, while *DEFL1*was present in the same tissues from LA1589pp and Sun1642pp (Fig. 4B). The expression of *SUN* in other vegetative parts of LA1589ee and Sun1642ee was at lower levels. We also detected a low level of *SUN* expression in the floral organs and roots of LA1589pp and Sun1642pp (Fig. 4). The expression of *SUN* in these tissues was presumably derived from the ancestral gene on chromosome 10.

The RNA in situ hybridization indicated that the expression pattern of *SUN* was ubiquitous throughout the ovary around the anthesis stage and young developing fruit, and not, as might have been expected, expressed at higher levels in septum tissues, where the morphology was changed most dramatically in the fruit of the NILs. Consistent with the previous studies (Xiao et al., 2008, 2009), our analyses showed *SUN* and *DEFL1* were expressed in similar tissue types and in a mutually exclusive manner. The latter result clearly demonstrated that the promoter of *DEFL1* was driving *SUN* expression on chromosome 7.

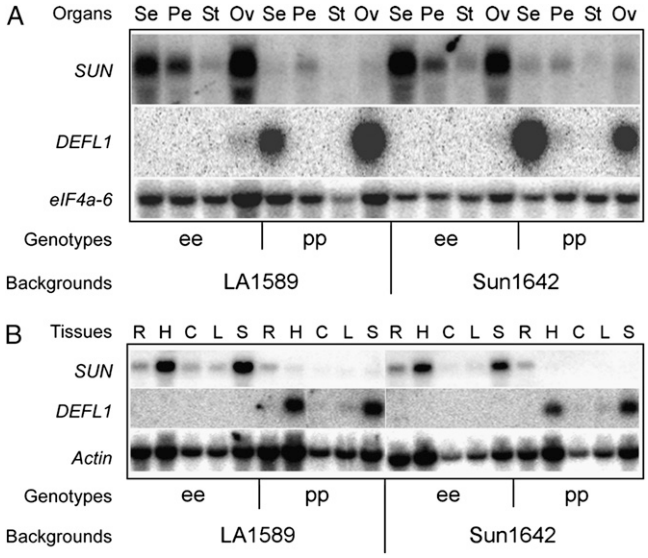

Figure 4. Expression patterns of *SUN* and *DEFL1* in floral organs and young seedlings of *sun* NILs. A, Expressions of *SUN* and *DEFL1* in floral organs of anthesis flowers. Se, Sepal; Pe, petal; St, stamen; Ov, ovary. B, Expressions of *SUN* and *DEFL1* in different tissues of young seedlings at 7 d post germination. R, Root; H, hypocotyl; C, cotyledon; L, leaf, S, shoot apex. ee, homozygous Sun1642 allele for *sun* locus; pp, homozygous LA1589 allele.

SUN Affects Lateral Organ Shapes

To determine whether *SUN* affects the shape of other floral organs, we evaluated stamen, petal, and sepal shape in the NILs that differ at *sun* in both Sun1642 and LA1589 backgrounds. As shown in Table III, sepals from LA1589ee and Sun1642ee were more elongated than those of LA1589pp and Sun1642pp. Stamen and petal shape was also altered but only significantly in the Sun1642 background (Table III). These results indicated that *SUN* controls floral organ shape in addition to fruit shape. Overexpression of *SUN* led to very elongated ovaries compared to the controls in both backgrounds (Fig. 5; Supplemental Fig. S2). Also, overexpression of *SUN* led to increased shape index of the other floral organs in both backgrounds (Table III). Moreover, in the LA1589 background the petals and stamens of *SUN* overexpressors were often fused with the ovary at the proximal end, suggesting a reduction in organ separation.

The effect of *SUN* on vegetative development was already noticeable shortly after seed germination (Fig. 6A). Lines that overexpress *SUN* showed dramatic effects on cotyledon and leaf shape (Fig. 6A). LA1589ee and Sun1642ee had slightly more elongated cotyledons than LA1589pp and Sun1642pp, and those of the *SUN* overexpressors were more slender and tapered at the distal end (Fig. 6, B and C; Table III). *SUN* did not affect leaflet number (Fig. 6, D and E), but higher levels of *SUN* expression led to altered leaflet margin characteristics (Fig. 6, B and C). In Sun1642 background, high levels of *SUN* expression were also associated with fusion between the rachis and the first pair of lateral leaflets, which were almost always found on the overexpressors and occasionally on Sun1642ee plants (Fig. 6D, inserts). We analyzed terminal leaflet shape based on the fifth true leaves on plants at 30 d after germination. The leaflet margin of the overexpressors was extremely serrated with an increased number of teeth and no proximal end indentation (Fig. 6, B and C; Table III; Supplemental Fig. S3A). However, the tooth numbers of terminal leaflets from the NILs were similar. The difference in regard to leaf margin feature between the NILs was that LA1589ee and Sun1642ee had more pointed tips, as well as a reduced proximal indentation area (Fig. 6, B and C; Table III). We also noticed that the shape indices of terminal leaflets from LA1589ee and Sun1642ee were higher and thus were more elongated than those of LA1589pp and Sun1642pp (Table III). Close-up views of vein structures showed *SUN* overexpressors had altered vein patterning with reduced angles between the secondary and tertiary vein and between the tertiary and quaternary veins (Supplemental Fig. S3B). It is conceivable that such changed vein structure was due to a less-expanded intervein area. In the overexpressors, more higher-order marginal veins ended freely in the lamina (Supplemental Fig. S3C), which could explain increased tooth number.

The leaves of the overexpressors were nearly always twisted in the rachis and petiole, often causing the leaflets to be positioned with the abaxial side facing upwards (Fig. 6, D and E). Cross sections of rachis taken between the first and second pairs of lateral leaflets showed that the rachis of overexpressors was much thinner (Fig. 7A). Although to a less extent, the leaf rachises in the LA1589ee and Sun1642ee were also twisted (Fig. 7, B and D). Closer inspections of the NILs revealed that the twisting rachis was associated with altered epidermal cell morphology. The abaxial epidermal cells tended to be less elongated and more disorganized in LA1589ee, Sun1642ee, and the *SUN* overexpressors compared to LA1589pp and Sun1642pp (Fig. 7, C and E). Disorderly arrangement of epidermal cells was also found in the adaxial side of the leaf rachises from LA1589ee and overexpressors in LA1589 background (Supplemental Fig. S4, A–C). The severe reduction in abaxial cell length could explain the downward curving of overexpressor leaf at an early developmental stage (Supplemental Fig. S4, D and E).

Table III. *Comparison of lateral organ shape and internode length in the NILs and lines overexpressing SUN*

L/W, Length-width ratio; nd, not determined.

Traits	LA1589 Background			*P* Value		Sun1642 Background			*P* Value	
	LA1589ee	LA1589pp	Overexpressor	pp versus ee	pp versus ox	Sun1642ee	Sun1642pp	Overexpressor	pp versus ee	pp versus ox
Sepal shape (L/W)	7.02 ± 0.38	5.57 ± 0.20	13.41 ± 0.92	<0.001	<0.001	9.75 ± 2.68	6.81 ± 0.73	25.89 ± 1.91	0.002	<0.001
Petal shape (L/W)	4.94 ± 0.22	4.71 ± 0.16	6.89 ± 0.13	0.107	<0.001	3.20 ± 0.84	2.86 ± 0.09	4.89 ± 0.49	0.012	0.003
Stamen shape (L/W)	6.09 ± 0.73	6.21 ± 0.58	7.35 ± 0.51	0.789	0.002	3.84 ± 1.00	3.28 ± 0.16	5.18 ± 0.41	0.005	<0.001
Ovary shape (L/W)	1.24 ± 0.06	1.15 ± 0.06	3.02 ± 0.89	0.036	<0.001	1.17 ± 0.31	1.05 ± 0.03	3.25 ± 0.66	<0.001	<0.001
Cotyledon shape (L/W)	4.95 ± 0.26	4.53 ± 0.31	8.41 ± 0.34	0.011	<0.001	3.63 ± 0.28	3.16 ± 0.31	5.99 ± 0.20	0.038	<0.001
Terminal leaflet shape (L/W)	2.31 ± 0.23	2.04 ± 0.08	2.16 ± 0.07	0.002	0.001	2.23 ± 0.15	1.76 ± 0.14	1.95 ± 0.06	0.001	0.077
Leaflet distal angle (degree)[a]	54.62 ± 1.79	64.60 ± 2.65	26.26 ± 2.76	0.008	<0.001	49.59 ± 1.43	58.83 ± 2.72	28.06 ± 1.86	0.017	<0.001
Leaflet proximal indentation[b]	0.046 ± 0.016	0.112 ± 0.013	0.002 ± 0.002	0.007	<0.001	0.008 ± 0.006	0.025 ± 0.011	0.000 ± 0.000	0.213	0.056
Hypocotyl length (cm)	2.93 ± 0.56	2.99 ± 0.55	nd	0.878	nd	3.65 ± 0.80	3.32 ± 0.59	nd	0.097	nd
Internode length (cm)	5.61 ± 1.21	6.27 ± 1.19	nd	0.106	nd	5.33 ± 0.53	5.45 ± 0.80	nd	0.685	nd

[a]The distal angle of leaflet was measured at the position of 10% above the tip by the Tomato Analyzer software. [b]The proximal indentation was evaluated by the indentation area relative to total fruit area.

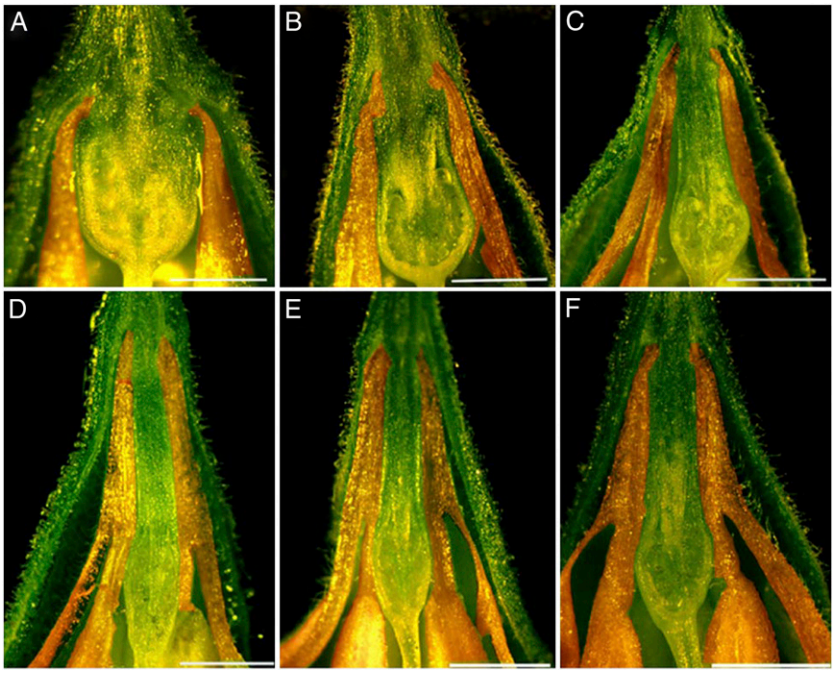

Figure 5. Ovary morphology of *SUN* overexpressors in LA1589 background. A, A wild-type anthesis ovary. B to F, Five anthesis ovaries of *SUN* overexpressors. Scale bars: 1 cm.

Overexpression of *SUN* Leads to Altered Plant Architecture

We did not observe significant alterations in overall plant growth between the *sun* NILs in both backgrounds, albeit that LA1589ee and Sun1642ee were slightly shorter than LA1589pp and Sun1642pp (Fig. 8, A and B). The shorter stature of LA1589ee and Sun1642ee was not due to decreased internode length (Table III), but changed internode angles, leading to zigzag stems. Overexpression of *SUN* caused dramatic changes in the architecture of the whole plant. These plants displayed prostrate growth and twisted stems (Fig. 8, A and B).

As mentioned above, Sun1642ee and *SUN* overexpressing plants had thinner and twisted leaf rachises (Fig. 7A). We further compared the stem morphologies among the NILs and *SUN* overexpressors in the Sun1642

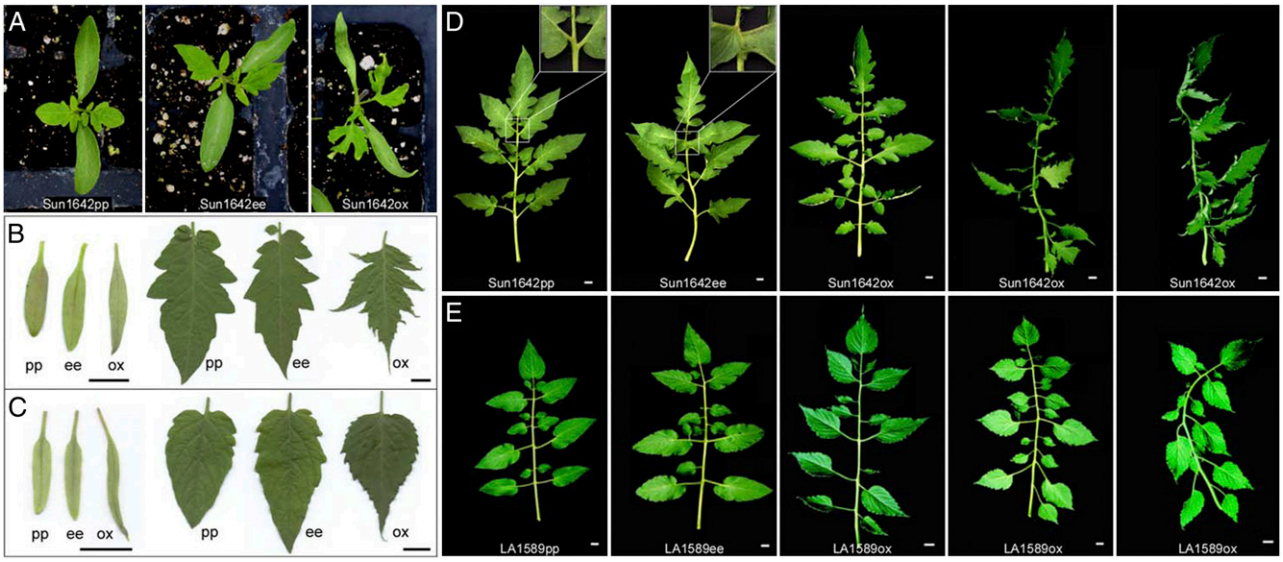

Figure 6. Leaf morphology of *sun* NILs and overexpressors. A, Seven days after germination seedlings of *sun* NILs and overexpressor in Sun1642 background. B, Cotyledons and terminal leaflets from *sun* NILs and overexpressor in Sun1642 background. C, Cotyledons and terminal leaflets from *sun* NILs and overexpressor in LA1589 background. D, Leaves of *sun* NILs and overexpressors in Sun1642 background. The inserts show the fusion between leaf rachis and leaflets in Sun1642ee, but not in Sun1642pp. E, Leaves of *sun* NILs and overexpressors in LA1589 background. Scale bars: 1 cm. [See online article for color version of this figure.]

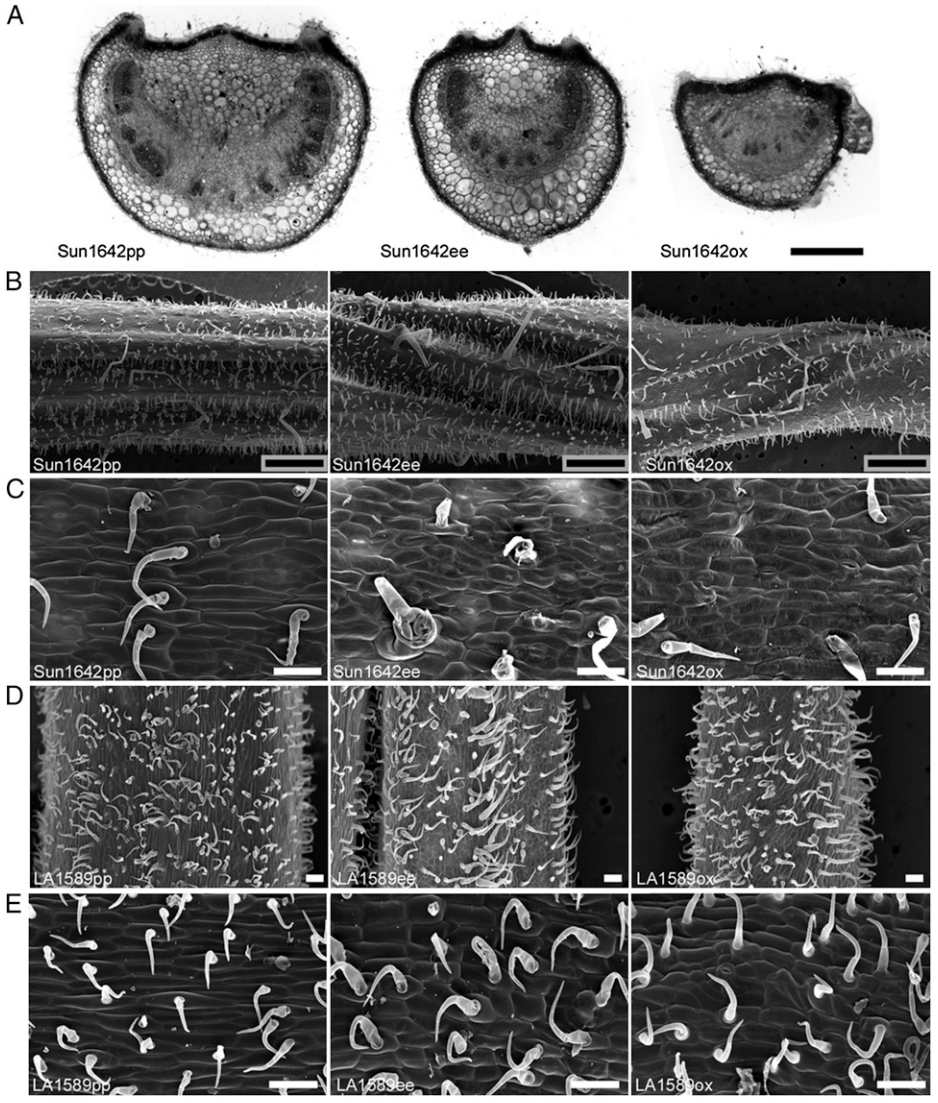

Figure 7. Leaf rachis of *sun* NILs and overexpressors. A, Cross sections of leaf rachis from *sun* NILs in Sun1642 background taken between the first and second pairs of lateral leaflets. B, Rachis from *sun* NILs and overexpressors in Sun1642 background. C, Rachis abaxial epidermal cells of *sun* NILs and overexpressors in Sun1642 background. D, Rachis from *sun* NILs and overexpressors in LA1589 background. E, Rachis abaxial epidermal cells of *sun* NILs and overexpressors in LA1589 background. Scale bars: black, 1 cm; white, 100 μm.

background. Cross sections of hypocotyls and stems at different positions were taken from 10- to 12-leaf-stage plants. We found altered stem anatomy in Sun1642ee and the overexpressors, especially the latter (Figs. 8C; Supplemental Fig. S5). The *SUN* overexpressing plants had reduced pith and more laterally expanded cortex cells compared to Sun1642pp (Fig. 8C). We also noticed that in the longitudinal direction, the cortex cells of Sun1642pp were arranged in several continuous strands, whereas those of the overexpressor were less elongated and disorganized (data not shown). A proposed helical growth model suggests this type of cortex cell morphology may underlie the twisting of the stem (Furutani et al., 2000; Ishida et al., 2007). Since the inner layer cells (cortex cells) have stronger isotropic expansion than the epidermal cells do, when there is a need to balance differences in longitudinal length, the outermost cell layer would tend to twist (Furutani et al., 2000; Ishida et al., 2007). In all, the stem phenotypes due to high *SUN* expression were similar to what we found in the leaf rachis and this could be explained by the helical growth model.

DISCUSSION

The locus *sun* was identified for its role in controlling tomato fruit shape (Van der Knaap and Tanksley, 2001; Xiao et al., 2008, 2009). In this study, using the NILs that differ at *sun* and *SUN* overexpressing lines, we further revealed that *SUN* is involved in controlling tomato fruit shape through redistribution of mass, and also plays important roles in the growth of other floral organs and in the vegetative development of the plant.

SUN Exerts Its Effect on Fruit Shape through a Change in Cell Division Patterns

The wild species accession LA1589 produces round and spherical fruits. The fruit of the *sun* NILs harbor-

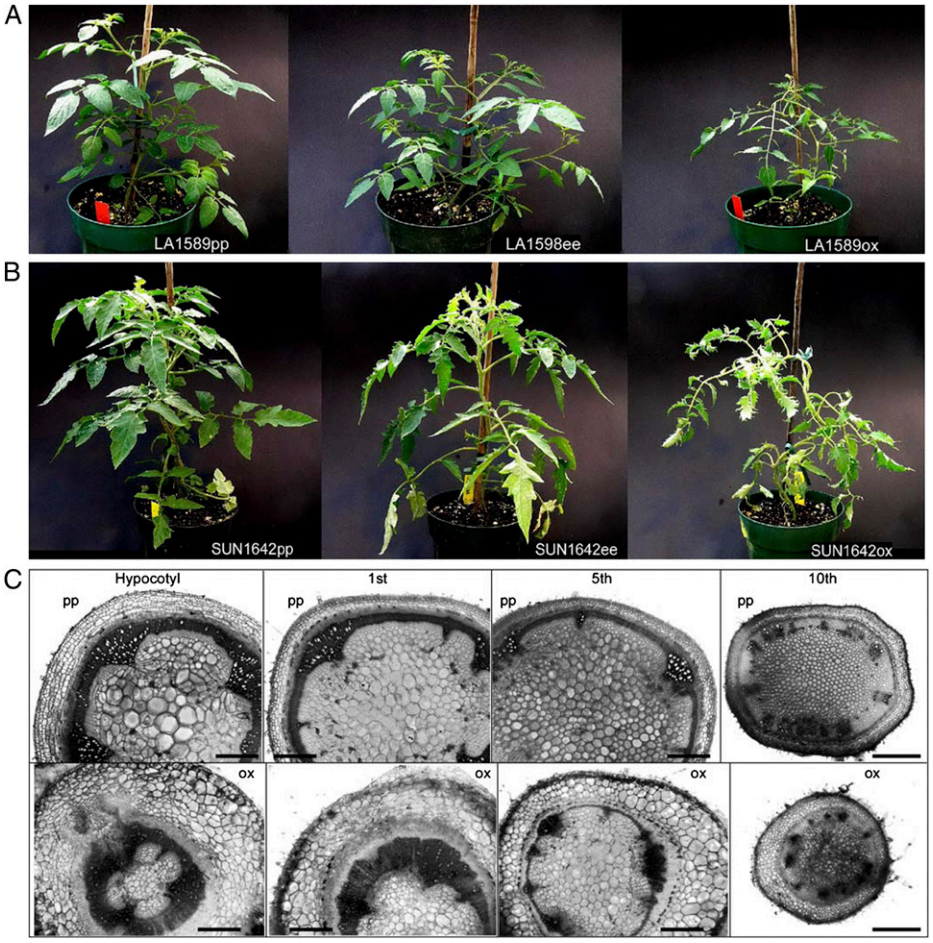

Figure 8. Plant shapes and stem morphology of *sun* NILs and overexpressors. A, Thirty days after germination plants of *sun* NILs and overexpressors in LA1589 background. B, Thirty days after germination plants of *sun* NILs and overexpressors in Sun1642 background. C, Cross sections of hypocotyls and stems from 12-leaf-stage Sun1642pp and Sun1642ox. Scale bars: 1 mm.

ing the elongated-fruited allele has increased length and reduced width compared to the fruit from the NILs having the round-fruited allele, suggesting that *SUN* promotes the longitudinal growth and decreases transverse growth. Since fruit weight is not affected by *SUN*, it is likely that it controls fruit shape through redistribution of mass. This proposed action of *SUN* on redirecting the dimensional growth of the fruit is supported by the observation that more cells were found in the longitudinal direction along the septum and pericarp of the 7-DPA fruits of LA1589ee, and fewer cells in the transverse direction (Table II; Fig. 2). Thus, *SUN* seems to induce the longitudinal cell division and to repress cell division in the transverse direction. We hypothesize that this is the result of a change of cell division planes.

SUN Affects Multiple Development Processes Reminiscent of Alterations in Auxin Transport

Ectopic expression of *SUN* under 35S promoter leads to fruit set without seed development. Production of pathenocarpic fruits can be triggered by exogenous application of plant hormone auxin or GA (de Jong et al., 2009a). Auxin and GA act synergistically in fruit initiation (Serrani et al., 2008; Vriezen et al., 2008), but they have different effects on parthenocarpic fruit growth in terms of ovule and locular tissue development (Serrani et al., 2007; de Jong et al., 2009a). The fruits of *SUN* overexpressors resemble the parthenocarpic fruits induced by auxin that have gel tissue filled in the locular cavities and produce pseudoembryos (de Jong et al., 2009a). It has been shown that inhibition of polar auxin transport (but not high auxin concentration) changes the orientation of cell division in tobacco (*Nicotiana tabacum*) cells (Petrásek et al., 2002; Campanoni et al., 2003). Thus, it is possible that *SUN* alters the axiality of cell division in tomato fruit by affecting, directly or indirectly, auxin transport.

In addition to fruit and leaf shape indices, *SUN* affects morphology by increasing serration at the leaflet margins (Fig. 5, B and C). In Arabidopsis, defining and positioning of teeth requires two key processes: polar auxin transport by PIN1 that creates local auxin maxima at the convergence points to allow serration outgrowth (Hay et al., 2006; Scarpella et al., 2006) and the activity of CUC2 in the sinus, leading to regional growth repression and/or extension of tooth outgrowth (Nikovics et al., 2006; Kawamura et al., 2010). *SUN* overexpressing plants have more teeth on the leaflets (Fig. 5, B and C; Supplemental Fig. S3), which could be the result of increased number of auxin maxima sites at the margin. Scarpella et al. (2006) found that more

convergence points in the epidermis can be promoted by exogenous auxin application. Therefore, it is possible that overexpressing *SUN* leads to high auxin levels in the marginal area of the leaflet. LA1589ee and Sun1642ee do not have more teeth on leaflets than LA1589pp and Sun1642pp, but reduce leaflet proximal end outgrowth and increase sinus indentation, which resemble the phenotypes caused by elevated activity of CUC2 and GOBLET in Arabidopsis and tomato, respectively (Nikovics et al., 2006; Berger et al., 2009). Auxin induces posttranscriptional repression of *CUC2* by activating *MIR164A* (Nikovics et al., 2006; Bilsborough et al., 2011). Our observation suggests *SUN* may play a role in disturbing normal auxin distribution in leaf, for example between tips (auxin maxima) and sinuses, and further affecting the activity of genes involved in leaf margin growth. Fusions between rachis and lateral leaflets (Fig. 6D), and at the proximal end of flower organs are also suggestive of perturbed auxin transport. Koenig et al. (2009) propose that during secondary morphogenesis, reduced auxin level and auxin response in tomato leaf rachis are necessary for preventing blade outgrowth along the rachis. Arrested polar auxin transport by *N*-1-naphthylphthalamic acid in maize (*Zea mays*) shoot also causes marginless leaf bases (Scanlon, 2003). Twisted leaf rachis and stem are indications that *SUN* could also affect auxin transport or response.

It has also been proposed that auxin distribution may underlie twisted growth in plants (Ishida et al., 2007). For example, twisting and asymmetric organ development of Arabidopsis mutants, *tornado1* (*trn1*), *trn2*, and *twisted dwarf1*, is accompanied by changed auxin transport patterns (Cnops et al., 2000; Bouchard et al., 2006; Cnops et al., 2006). Since *SUN* expression does not lead to differences in expression of auxin signaling and biosynthesis-related genes (Xiao et al., 2009), and considering the fruit and vegetative phenotypes discussed above, it is conceivable that if *SUN* interacts with the auxin pathway, this is more likely via altering auxin transport than auxin signaling.

MATERIALS AND METHODS

Plant Materials

NILs were developed from crosses between tomato (*Solanum lycopersicum*) var. Sun1642 and the wild species *Solanum pimpinellifolium* LA1589, to ensure a small introgression of approximately 60 kb (Xiao et al., 2008). Recombinants with small introgressions were identified during the positional cloning of the gene and facilitated by the high recombination rate around the locus. The resulting two sets of NILs were used for phenotypic analysis. The *SUN* overexpressors in LA1589 genetic background were described previously, and *SUN* overexpressors in Sun1642 background were obtained by transforming pEK69 into round-fruited NIL Sun1642pp as described previously (Xiao et al., 2008). Transgenic plants and LA1589 *sun* NILs were grown in greenhouse, whereas Sun1642 NILs were grown in greenhouse and fields in Wooster, OH.

Phenotypic Analysis

Flower and Fruit Measurements

Fruit measurements were taken of eight to 10 fruits per plant. Ten or more measurements were taken for other morphological traits. To ensure sufficient seed set, open flowers were tagged and hand pollinated. Anthesis-staged flowers were used for measurement of floral organ shapes. Different floral organs were dissected and images were taken under a dissection microscope (NILs and overexpressors in LA1589 background) or by scanner (NILs and overexpressors in Sun1642 background). The organ shapes were measured by ImageJ (http://rsb.info.nih.gov/ij/) on the images taken. Mature fruit shape was measured by TomatoAnalyzer (Brewer et al., 2006; http://www.oardc.ohio-state.edu/vanderknaap/tomato_analyzer.htm). Seed numbers were counted per fruit, and 100 seeds were weighed for seed weight.

Leaf Measurements

For internode length, leaflet shape, and leaflet number, three measurements were conducted on each plant of a total of five plants for each genotype. Terminal leaflet shape index and distal angle were measured by TomatoAnalyzer (Brewer et al., 2006). The leaf shape index refers to the ratio of height to width, and the distal angle of leaflet was measured at the position of 10% above the tip. For cotyledon shape analysis of NILs and overexpressors, cotyledons were collected from two- to three-leaf-stage seedlings. For leaflet vein morphology, terminal leaflets from wild-type plants and overexpressors were fixed in Carnoy's fluid containing acetic acid, absolute ethanol, and chloroform (1:6:3 by volume). Images were taken by scanner.

Hypocotyl and Stem Sectioning

Hypocotyl and stem cross sections were taken from the middle of hypocotyls and between subsequent nodes of 12-leaf-stage NILs and overexpressors in Sun1642 background. Fresh-cut 300-μm-thick sections were made using the 4000 automatic oscillating tissue slicer (Electron Microscopy Sciences). Sections were stained with 0.5% toluidine blue for a few minutes and washed with water. Images were then taken using a dissecting microscope (Leica MZFLIII) equipped with the Spot RTKE 7.2 color mosaic camera.

Scanning Electron Microscopy

Leaf rachises of the sixth leaves and lateral shoots were collected from 4-week-old plants. Hand-pollinated fruits of the *sun* NILs in LA1589 background were harvested at 7 d after pollination. The fruits were sliced through the middle in the longitudinal or transverse direction. All samples were immediately infiltrated and fixed with 3% gluteraldehyde, 2% paraformaldehyde in 0.1 M potassium phosphate buffer pH 7.4 for 2 h at room temperature, and then overnight at 4°C. Samples were then washed four times with phosphate buffer and dehydrated through an ethanol series, critical point dried, mounted, and coated with platinum as described previously (Xiao et al., 2009). Samples were viewed and images recorded with a Hitachi 3500N scanning electron microscope (Hitachi High Technologies America, Inc.) under high vacuum. Cell counting and measurements were done on the scanning electron microscopy micrographs using ImageJ software.

Northern Blot

Total RNA for various tomato tissues were extracted using Trizol reagent (Invitrogen Inc.) as previously described (Xiao et al., 2008). In all RNA preparations, tissues were quickly frozen in liquid nitrogen after harvest and then stored in freezer (−80°C) until RNA extraction. Ten micrograms of total RNA per sample was separated in 1.2% agarose gel in 1× MOPS buffer containing formaldehyde, then transferred to Hybond N membrane (Amersham Biosciences). Hybridizations were performed at 42°C in formamide-containing hybridization buffer sequentially with radiolabeled gene-specific probes as previously described (Xiao et al., 2008). *eIF4α6* or actin were used as loading controls.

In Situ Hybridization

RNA in situ hybridization was performed using the protocol reported by Balasubramanian and Schneitz (2002) with minor modification. To generate RNA probes for in situ hybridization, we amplified linear templates for *SUN*

and *DEFL1* from cDNA using following primers: *SUN*, 5′-ATGGGAAAGCGAAGAAAC-3′ and 5′-AATAGCAGCTTGTTTGCGTT-3′ and *DEFL1*, 5′-GGCACAATCCATTCGTTTCT-3′ and 5′-GTCTAGTGCACCATAATTGC-3′. An antisense or sense RNA probe was created by adding a sequence containing the T7 promoter to the 5′ of the reverse or forward primer, respectively. Probes were labeled by in vitro transcription with T7 polymerase using a digoxigenin (DIG) RNA labeling kit (Roche). Flowers at 9 and 4 d before anthesis were vacuum infiltrated and fixed with 4% paraformaldehyde in 1× phosphate-buffered saline pH 7.0. Samples were washed with 1× phosphate-buffered saline, dehydrated with ethanol series and histoclear, and finally infiltrated and embedded in paraffin (Polyscience). Ten-microgram sections were taken with a microtome (American Optical Spencer 820). Sections were deparaffinized and rehydrated before acetylation, and then dehydrated. The slides were hybridized overnight with DIG-labled RNA probes at 55°C, and washed with 0.2× saline-sodium citrate buffer and blocked with blocking solution (Boehringer). DIG-labeled RNA was detected by alkaline phosphatase-conjugated antibody (Anti-Digoxigenin-AP Fab fragments, Roche). The antibody (1:1,000) was applied to the slides, incubated at room temperature, and washed off, followed by color reaction with 4-nitro-blue-tetrazolium-chloride/5-bromo-4-chloro-3-indolyl-phosphate solution (Roche). The slides were mounted and sealed. The images were taken using a microscope (Leica DM IRB) equipped with a digital camera (Q Imaging Retiga 2000).

Supplemental Data

The following materials are available in the online version of this article.

Supplemental Figure S1. Expressions of *SUN* and *DEFL1* mRNA in 6-DPA fruits of *sun* NILs in the LA1589 background.

Supplemental Figure S2. Ovary morphology of *SUN* overexpressors in Sun1642 background.

Supplemental Figure S3. Vein patterns of terminal leaflets from wild type and *SUN* overexpressing plants in LA1589 background.

Supplemental Figure S4. Epidermal cell morphology of leaf rachises from *sun* NILs and overexpressors.

Supplemental Figure S5. Hypocotyl and stem morphology of 12-leaf-stage *sun* NILs and overexpressors in Sun1642 background.

Supplemental Table S1. Comparison of fruit components between pHX4 transgenic lines in LA1589 background.

Supplemental Table S2. Light microscopy analysis of anthesis ovaries from the LA1589 *sun* NILs.

ACKNOWLEGDMENTS

We thank Dr. R. Lamb and Dr. J.C. Jang for helpful comments and Ms. A. Kaszas of the Molecular and Cellular Imaging Center at Ohio State University, Wooster for help with the microscopy.

Received June 8, 2011; accepted September 8, 2011; published September 15, 2011.

LITERATURE CITED

Abel S, Savchenko T, Levy M (2005) Genome-wide comparative analysis of the IQD gene families in *Arabidopsis thaliana* and *Oryza sativa*. BMC Evol Biol **5:** 72

Alonso-Cantabrana H, Ripoll JJ, Ochando I, Vera A, Ferrándiz C, Martínez-Laborda A (2007) Common regulatory networks in leaf and fruit patterning revealed by mutations in the Arabidopsis *ASYMMETRIC LEAVES1* gene. Development **134:** 2663–2671

Balasubramanian S, Schneitz K (2002) NOZZLE links proximal-distal and adaxial-abaxial pattern formation during ovule development in *Arabidopsis thaliana*. Development **129:** 4291–4300

Berger Y, Harpaz-Saad S, Brand A, Melnik H, Sirding N, Alvarez JP, Zinder M, Samach A, Eshed Y, Ori N (2009) The NAC-domain transcription factor GOBLET specifies leaflet boundaries in compound tomato leaves. Development **136:** 823–832

Bilsborough GD, Runions A, Barkoulas M, Jenkins HW, Hasson A, Galinha C, Laufs P, Hay A, Prusinkiewicz P, Tsiantis M (2011) Model for the regulation of *Arabidopsis thaliana* leaf margin development. Proc Natl Acad Sci USA **108:** 3424–3429

Bouchard R, Bailly A, Blakeslee JJ, Oehring SC, Vincenzetti V, Lee OR, Paponov I, Palme K, Mancuso S, Murphy AS, et al (2006) Immunophilin-like TWISTED DWARF1 modulates auxin efflux activities of Arabidopsis P-glycoproteins. J Biol Chem **281:** 30603–30612

Brewer MT, Lang L, Fujimura K, Dujmovic N, Gray S, van der Knaap E (2006) Development of a controlled vocabulary and software application to analyze fruit shape variation in tomato and other plant species. Plant Physiol **141:** 15–25

Campanoni P, Blasius B, Nick P (2003) Auxin transport synchronizes the pattern of cell division in a tobacco cell line. Plant Physiol **133:** 1251–1260

Cnops G, Neyt P, Raes J, Petrarulo M, Nelissen H, Malenica N, Luschnig C, Tietz O, Ditengou F, Palme K, et al (2006) The *TORNADO1* and *TORNADO2* genes function in several patterning processes during early leaf development in *Arabidopsis thaliana*. Plant Cell **18:** 852–866

Cnops G, Wang X, Linstead P, Van Montagu M, Van Lijsebettens M, Dolan L (2000) *Tornado1* and *tornado2* are required for the specification of radial and circumferential pattern in the Arabidopsis root. Development **127:** 3385–3394

Coen E (2001) Goethe and the ABC model of flower development. C R Acad Sci III **324:** 523–530

de Jong M, Mariani C, Vriezen WH (2009a) The role of auxin and gibberellin in tomato fruit set. J Exp Bot **60:** 1523–1532

de Jong M, Wolters-Arts M, Feron R, Mariani C, Vriezen WH (2009b) The *Solanum lycopersicum* auxin response factor 7 (*SlARF7*) regulates auxin signaling during tomato fruit set and development. Plant J **57:** 160–170

Furutani I, Watanabe Y, Prieto R, Masukawa M, Suzuki K, Naoi K, Thitamadee S, Shikanai T, Hashimoto T (2000) The *SPIRAL* genes are required for directional control of cell elongation in Arabidopsis thaliana. Development **127:** 4443–4453

Goethe JW (1970) Italian Journey. Penguin Classics, London

Hay A, Barkoulas M, Tsiantis M (2006) *ASYMMETRIC LEAVES1* and auxin activities converge to repress *BREVIPEDICELLUS* expression and promote leaf development in Arabidopsis. Development **133:** 3955–3961

Honma T, Goto K (2001) Complexes of MADS-box proteins are sufficient to convert leaves into floral organs. Nature **409:** 525–529

Ishida T, Thitamadee S, Hashimoto T (2007) Twisted growth and organization of cortical microtubules. J Plant Res **120:** 61–70

Jiang N, Gao D, Xiao H, van der Knaap E (2009) Genome organization of the tomato *sun* locus and characterization of the unusual retrotransposon *Rider*. Plant J **60:** 181–193

Jones B, Frasse P, Olmos E, Zegzouti H, Li ZG, Latché A, Pech JC, Bouzayen M (2002) Down-regulation of DR12, an auxin-response-factor homolog, in the tomato results in a pleiotropic phenotype including dark green and blotchy ripening fruit. Plant J **32:** 603–613

Kawamura E, Horiguchi G, Tsukaya H (2010) Mechanisms of leaf tooth formation in Arabidopsis. Plant J **62:** 429–441

Koenig D, Bayer E, Kang J, Kuhlemeier C, Sinha N (2009) Auxin patterns *Solanum lycopersicum* leaf morphogenesis. Development **136:** 2997–3006

Levy M, Wang Q, Kaspi R, Parrella MP, Abel S (2005) Arabidopsis IQD1, a novel calmodulin-binding nuclear protein, stimulates glucosinolate accumulation and plant defense. Plant J **43:** 79–96

Molesini B, Pandolfini T, Rotino GL, Dani V, Spena A (2009) Aucsia gene silencing causes parthenocarpic fruit development in tomato. Plant Physiol **149:** 534–548

Nikovics K, Blein T, Peaucelle A, Ishida T, Morin H, Aida M, Laufs P (2006) The balance between the *MIR164A* and *CUC2* genes controls leaf margin serration in *Arabidopsis*. Plant Cell **18:** 2929–2945

Østergaard L (2009) Don't 'leaf' now: the making of a fruit. Curr Opin Plant Biol **12:** 36–41

Paran I, van der Knaap E (2007) Genetic and molecular regulation of fruit and plant domestication traits in tomato and pepper. J Exp Bot **58:** 3841–3852

Pelaz S, Tapia-López R, Alvarez-Buylla ER, Yanofsky MF (2001) Conversion of leaves into petals in Arabidopsis. Curr Biol **11:** 182–184

Petrásek J, Elckner M, Morris DA, Zazímalová E (2002) Auxin efflux carrier activity and auxin accumulation regulate cell division and polarity in tobacco cells. Planta **216:** 302–308

Scanlon MJ (2003) The polar auxin transport inhibitor N-1-naphthyl-

phthalamic acid disrupts leaf initiation, KNOX protein regulation, and formation of leaf margins in maize. Plant Physiol **133:** 597–605

Scarpella E, Marcos D, Friml J, Berleth T (2006) Control of leaf vascular patterning by polar auxin transport. Genes Dev **20:** 1015–1027

Serrani JC, Ruiz-Rivero O, Fos M, García-Martínez JL (2008) Auxin-induced fruit-set in tomato is mediated in part by gibberellins. Plant J **56:** 922–934

Serrani JC, Sanjuán R, Ruiz-Rivero O, Fos M, García-Martínez JL (2007) Gibberellin regulation of fruit set and growth in tomato. Plant Physiol **145:** 246–257

Van der Knaap E, Tanksley SD (2001) Identification and characterization of a novel locus controlling early fruit development in tomato. Theor Appl Genet **103:** 353–358

Vriezen WH, Feron R, Maretto F, Keijman J, Mariani C (2008) Changes in tomato ovary transcriptome demonstrate complex hormonal regulation of fruit set. New Phytol **177:** 60–76

Wang H, Jones B, Li Z, Frasse P, Delalande C, Regad F, Chaabouni S, Latché A, Pech JC, Bouzayen M (2005) The tomato Aux/IAA transcription factor IAA9 is involved in fruit development and leaf morphogenesis. Plant Cell **17:** 2676–2692

Xiao H, Jiang N, Schaffner EK, Stockinger EJ, van der Knaap E (2008) A retrotransposon-mediated gene duplication underlies morphological variation of tomato fruit. Science **319:** 1527–1530

Xiao H, Radovich C, Welty N, Hsu J, Li D, Meulia T, van der Knaap E (2009) Integration of tomato reproductive developmental landmarks and expression profiles, and the effect of *SUN* on fruit shape. BMC Plant Biol **9:** 49